Insights into Pyrolysis Kinetic, Thermodynamics, and Reaction Mechanism of Wheat Straw for Its Bioenergy Potential

Jialiu Lei *, Xiaofeng Ye , Han Wang , Dongnan Zhao

Posted Date: 26 June 2023

doi: 10.20944/preprints202306.1739.v1

Keywords: pyrolysis behavior; thermogravimetric analysis; kinetics and thermodynamics; reaction mechanism; wheat straw

Article

Insights into Pyrolysis Kinetic, Thermodynamics, and Reaction Mechanism of Wheat Straw for Its Bioenergy Potential

JialiuLei [1,2,*], Xiaofeng Ye [1], Han Wang [1] and Dongnan Zhao [1]

[1] School of Materials Science and Engineering, Hubei Polytechnic University, Huangshi 435003, China; zhaodongnan@hbpu.edu.cn (D.Z.); yexiaofeng@stu.hbpu.edu.cn (X.Y.); wanghan@stu.hbpu.edu.cn (H.W.)

[2] The State Key Laboratory of Refractories & Metallurgy, Wuhan University of Science and Technology, Wuhan 430081, China

* Correspondence: leijialiu@hbpu.edu.cn (J.L.); Tel.: +86-0714-635-8328

Abstract: To realize the energy recovery of wheat straw, the pyrolysis behavior of wheat straw was studied at three heating rates (10, 20, and 30 K/min) based on thermogravimetric analysis (TG–DTG). Kinetics and thermodynamics were analyzed using Flynn–Wall–Ozawa (FWO) and Kissinger–Akahira–Sunose (KAS) model-free methods, and reaction mechanism was determined using Coats–Redfern (CR) model-fitting method. The results show that there are three weightlessness stages in the pyrolysis process, of which the second stage was the main weightlessness stage and two distinct peaks of weightlessness were observed in this stage. With increasing heating rate, the main pyrolytic weightlessness peaks of DTG curve shifts to higher temperature. The pyrolysis activation energy calculated by FWO and KAS methods are 165.17–440.02 kJ/mol and 163.72–452.07 kJ/mol, and the pre-exponential factor vary in the range of 2.58×10^{12}–7.45×10^{36} s^{-1} and 1.91×10^{12}–8.66×10^{37} s^{-1}, respectively. The thermodynamic parameters indicates that wheat straw has the favorable conditions for product formation and containes potential energy to be utilized for bioenergy production, its pyrolysis reaction was non-spontaneous and the energy output is stable. CR method analysis shows that the $A_{1/3}$ random nucleation model is the most suitable mechanism to characterize the pyrolysis process, and random nucleation may be in charge of the main pyrolysis stage. This study can provide a theoretical basis for the thermochemical conversion and utilization of wheat straw.

Keywords: pyrolysis behavior; thermogravimetric analysis; kinetics and thermodynamics; reaction mechanism; wheat straw

1. Introduction

With the rapid development of social economy and technology, the excessive use of fossil energy has brought great disasters to the environment. Global warming, environmental pollution, energy shortage and other issues have attracted high attention from the scientific community [1]. With the gradual depletion of fossil fuels, more and more attentions were paid to the renewable energy. The biomass become the most potential renewable energy sources due to its "carbon neutral" feature [2], and considered as the most promising alternative with the potential to abate carbon emissions. It can be converted into biomass gas, biochar, liquid fuels, and high value-added chemical raw materials through the thermochemical process [3]. The biomass gas can be used as a gaseous biofuel for power generation, and the liquid fraction can be used as biofuel after upgrading [4,5]. The biochar is mostly composed of carbon and inorganic materials, which can be applied as soil amendment [6,7]. Biomass includes agricultural residues and forest residues, as the world's major agricultural country, the crop straw output reaches about 910 million tons in China per year, among which the wheat straw production reaches about 300 million tons. Its enormous output and ready availability make it extensively used as a fuel in China. However, traditional utilization of wheat straw by simple combustion techniques often result in low combustion efficiency and high carbon emissions. Meanwhile, pyrolysis causes less pollution emission, and has a reasonable cost and simple operation, making it become the most basic thermochemical transformation process. Therefore, the study of

 doi:10.20944/preprints202306.1739.v1

pyrolysis is helpful to effectively control the thermochemical transformation process, and the insights into kinetic, thermodynamic parameters, and reaction mechanism are the key to the design of large-scale pyrolysis reactor [8,9]. Through optimizing the pyrolysis process parameters, it is expected to maximize the yield of target products.

Thermogravimetric analysis (TGA) is a common method for understanding pyrolysis behavior and studying pyrolysis kinetics of wheat straw. Based on the thermogravimetric data, the reaction mechanism function and related kinetic parameters can be obtained. Currently, the study on biomass pyrolysis process mainly include model-fitting and model-free methods [10–13]. The activation energy obtained from model-free methods is more reliable since there is no need to assume reaction mechanism functions. Model-fitting methods can calculate both activation energy and pre-exponential factor with an assumption of reaction mechanism function. Thus, model-free methods and model-fitting methods should support with each other to calculate kinetic parameters, and investigate the reaction mechanism [14].

In order to provide a theoretical basis for the utilization of wheat straw and then provide a guidance for the development of large-scale pyrolysis reactor. In this work, the wheat straw was subjected to TGA at different heating rates with an aim to understand the pyrolytic behavior with reaction mechanism. The kinetic and thermodynamics parameters of different pyrolysis processes were obtained by the recommended model-free models of Flynn–Wall–Ozawa (FWO) and Kissinger–Akahira–Sunose (KAS) [15–17], and the reaction mechanism for the pyrolysis process was determined by the Coats–Redfern (CR) model-fitting method [18,19].

2. Materials and Methods

2.1. Materials

The wheat straw used in this experiment was ground and sieved to pass through a 150-mesh screen. The proximate analysis and ultimate analysis of wheat straw were conducted using the Chinese standard. As shown in Table 1, the content of C and O elements in wheat straw are the highest and the content of S and N elements are the least. The C and H elements have a great influence on the calorific value of fuel and lower N and S content result in the lower emission of NOx and SOx in the atmosphere. The results of proximate analysis show that the volatile content is as high as 67.88%, the fixed carbon content is 15.07%, and the ash content is only 8.33%. Low ash content is conducive to the improvement of heat transfer efficiency during the pyrolysis process, while high volatile content and high fixed carbon content are helpful to the improvement of fuel performance.

Table 1. Proximate analysis and ultimate analysis of wheat straw.

Proximate analysis /%				Ultimate analysis /%				
Moisture	Ash	Volatiles	Fixed carbon	N	C	H	S	O
8.72	8.33	67.88	15.07	1.12	41.42	6.06	0.53	41.78

2.1.1. FTIR analysis

In order to understand the functional groups of wheat straw, the FTIR analysis was carried out. The spectra were collected within the wavenumber range of 400–4000 cm^{-1} as shown in Figure 1. The absorption peak at 3405 cm^{-1} is due to –OH stretching, which ascribed to cellulose and lignin [20], while the sharp absorption peak at 2919 cm^{-1} and 2852 cm^{-1} are mainly caused by the asymmetric and symmetric stretching vibration of $–CH_2$. The absorption peak at 1656 cm^{-1} is the stretching vibration of conjugated carbonyl C=O, and the peak at 1247 cm^{-1} is attributed to the stretching vibration of C–O. The absorption peak at 1162 cm^{-1} is the antisymmetric stretching vibration of the C–O–C glycosioside bond contained in cellulose and hemicelluellulost [21], and the absorption peak at 1050 $cm^{-1}$is the stretching vibration of primary alcohol C–O [22].

Preprints (www.preprints.org) | NOT PEER-REVIEWED | Posted: 26 June 2023 doi:10.20944/preprints202306.1739.v1

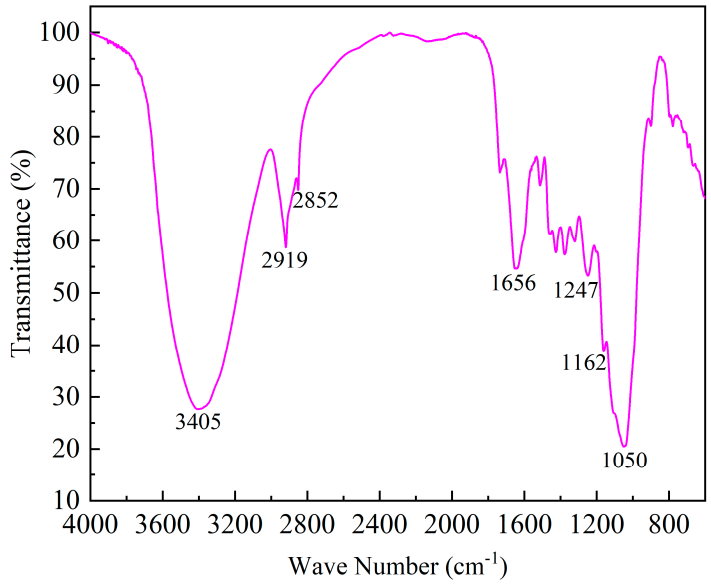

Figure 1. FTIR spectrum of wheat straw.

2.1.2. SEM analysis

The scanning electron microscope (SEM) morphology analysis of wheat straw is shown in Figure 2. As can be seen, the wheat straw sample presents an irregular rod-like shape with fibrous flakes on its surface without no pores. Some nano adsorption particles can be clearly seen on the surface.

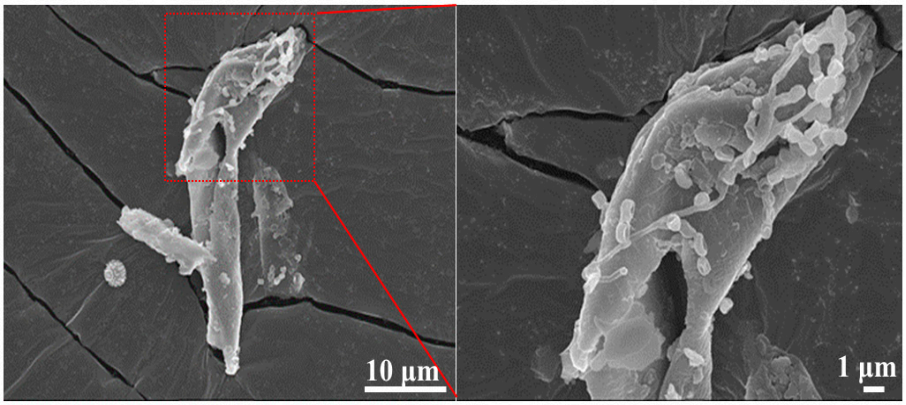

Figure 2. Micromorphology of wheat straw.

2.2. Experimental procedure

Thermogravimetric testing was performed using TGA5500 thermogravimetric analyzer. The mass of each sample weighing about 8 mg was placed in the alumina crucible, and then heated from room temperature to 1,173 K. The mass, time, temperature, and other signals of sample were recorded online by computer program. High purity nitrogen with purity of 99.999% was used during the whole pyrolysis process. The gas flow rate was 60 mL/min, and the heating rates were 10, 20, and 30 K/min, respectively. The experiment of each heating rate was repeated three times to ensure the accuracy of the experiment within the error range of ±3%. Before the experiment, the samples were placed in a drying oven of 383 K for 12 h.

2.3. Kinetic method

Pyrolysis of biomass is a complex reaction. The thermal reaction in the pyrolysis process follows the following reaction: A(solid)→B(solid)+C(gas). For a non-isothermal and heterogeneous reaction, the conversion rate of biomass pyrolysis can be expressed in the following Equation [23].

Preprints (www.preprints.org) | NOT PEER-REVIEWED | Posted: 26 June 2023 doi:10.20944/preprints202306.1739.v1

$$\frac{d\alpha}{dt} = k(T)f(\alpha) \quad (1)$$

Where α is the conversion rate, t is the pyrolysis time, $k(T)$ is the pyrolysis reaction rate constant, $f(\alpha)$ is the differential expression of the kinetic mechanism function. The α can be calculated from the data obtained by thermogravimetric analysis, as shown in Equation (2).

$$\alpha = \frac{m_0 - m_t}{m_0 - m_\infty} \quad (2)$$

Where m_0, m_t, and m_∞ represent the initial mass of biomass,mass of biomass at time t, and final mass of biomass, respectively.

According to Arrhenius law, k(T) can be represented by the Equation (3).

$$k(T) = A\exp\left(-\frac{E}{RT}\right) \quad (3)$$

Where T represents the reaction temperature (K), A is the pre-exponential factor (1/s), E is the activation energy (kJ/mol), and R represents the universal gas constant (8.314 J/mol/K).

When the temperature rises at a given rate (β=dT/dt), the Equation (3) can be obtained as follows:

$$\frac{d\alpha}{dT} = \frac{A}{\beta}\exp\left(-\frac{E}{RT}\right)f(\alpha) \quad (4)$$

The integrated form of $f(\alpha)$ is generally expressed as:

$$\int_0^\alpha \frac{d\alpha}{f(\alpha)} = g(\alpha) = \frac{A}{\beta}\int_{T_0}^{T} e^{-\frac{E}{RT}}\,dT \quad (5)$$

2.3.1. Model-free methods

In order to analyze the kinetic parameters, two model-free methods of Flynn–Wall–Ozawa (FWO) and Kissinger–Akahira–Sunose (KAS) were employed in this work.

The FWO method can be expressed as Equation (6) [24], there is a linear relationship between ln(β) and 1/T at different heating rates β. The activation energy of pyrolysis can be calculated from the slope −1.052E/R of the fitting equation .

$$\ln\beta = \ln\frac{AE}{g(\alpha)R} - 5.331 - 1.052\frac{E}{RT} \quad (6)$$

The KAS method can be written as Equation (7) [25], there is a linear relationship between ln(β/T^2) and 1/T at different heating rates β. The pyrolysis activation energy can be obtained from the slope −E/R of the fitting equation.

$$\ln\frac{\beta}{T^2} = \ln\frac{AE}{g(\alpha)R} - \frac{E}{RT} \quad (7)$$

2.3.2. Model-fitting methods

The model-fitting methods took the reaction mechanism function into consideration, which can help to obtain the fittest reaction mechanism function. In this study, the reaction mechanism was studied by Coats–Redfern (CR) method [26,27], which is derived from the Arrhenius equation as follows.

$$\ln\frac{g(\alpha)}{T^2} = \ln\frac{AR}{\beta E} - \frac{E}{RT} \quad (8)$$

The E can be calculated by plotting ln$g(\alpha)$/T^2 versus 1/T in terms of the algebraic expressions for $g(\alpha)$. If the average E value acquired by model fitting method (CR method in this study) with a given kinetic model is consistent with that calculated by model-free methods (FWO and KAS), the corresponding reaction model may be utilized to describe the thermal decomposition process. The

Preprints (www.preprints.org) | NOT PEER-REVIEWED | Posted: 26 June 2023 doi:10.20944/preprints202306.1739.v1

reaction mechanisms of biomass pyrolysis are broadly classified into five major categories, namely diffusion, chemical reaction order, random nucleation, diffusional, phase boundary reaction, and exponential nucleation. In this study, 20 common pyrolysis reaction models were selected in five categories of reaction mechanisms, which are listed in Table 2 [28–30].

Table 2. Common solid-state thermal reaction mechanisms.

Mechanism	symbol	$f(\alpha)$	$g(\alpha)$
Diffusion	D	Differential form	Integral form
One-way transport	D_1	$1/2\,\alpha$	α^2
Two-way transport	D_2	$[-\ln(1-\alpha)]^{-1}$	$\alpha+(1-\alpha)\ln(1-\alpha)$
Three-way transport	D_3	$[(3/2)(1-\alpha)^{2/3}]/[1-(1-\alpha)^{1/3}]$	$[1-(1-\alpha)^{1/3}]^2$
Ginstling-Brounshtein	D_4	$(3/2)[(1-\alpha)^{1/3}-1]^{-1}$	$(1-2\alpha/3)-(1-\alpha)^{2/3}$
Zhuravlev,Lesokin,Tempelman	D_5	$[(3/2)(1-\alpha)^{4/3}]/[(1-\alpha)^{-1/3}-1]$	$[(1-\alpha)^{-1/3}-1]^2$
Chemical reaction order	F	Differential form	Integral form
First-order	F_1	$1-\alpha$	$-\ln(1-\alpha)$
Second-order	F_2	$(1-\alpha)^2$	$(1-\alpha)^{-1}-1$
Third-order	F_3	$(1-\alpha)^3$	$[(1-\alpha)^{-2}-1]/2$
Random nucleation	A	Differential form	Integral form
Avrami-Erofeyev(*n*=2)	A_2	$2(1-\alpha)[-\ln(1-\alpha)]^{1/2}$	$[-\ln(1-\alpha)]^{1/2}$
Avrami-Erofeyev(*n*=3)	A_3	$3(1-\alpha)[-\ln(1-\alpha)]^{2/3}$	$[-\ln(1-\alpha)]^{1/3}$
Avrami-Erofeyev(*n*=4)	A_4	$4(1-\alpha)[-\ln(1-\alpha)]^{3/4}$	$[-\ln(1-\alpha)]^{1/4}$
Avrami-Erofeyev(*n*=1/2)	$A_{1/2}$	$1/2(1-\alpha)[-\ln(1-\alpha)]^{-1}$	$[-\ln(1-\alpha)]^2$
Avrami-Erofeyev(*n*=1/3)	$A_{1/3}$	$1/3(1-\alpha)[-\ln(1-\alpha)]^{-2}$	$[-\ln(1-\alpha)]^3$
Avrami-Erofeyev(*n*=1/4)	$A_{1/4}$	$1/4(1-\alpha)[-\ln(1-\alpha)]^{-3}$	$[-\ln(1-\alpha)]^4$
Phase boundary reaction	R	Differential form	Integral form
Contracting disk	R_1	1	α
Contracting cylinder	R_2	$2(1-\alpha)^{1/2}$	$1-(1-\alpha)^{1/2}$
Contracting sphere	R_3	$3(1-\alpha)^{2/3}$	$1-(1-\alpha)^{1/3}$
Exponential nucleation	P	Differential form	Integral form
Power law (n = 1 /2)	$P_{1/2}$	$2\alpha^{1/2}$	$\alpha^{1/2}$
Power law (n = 1 /3)	$P_{1/3}$	$3\alpha^{2/3}$	$\alpha^{1/3}$
Power law (n = 1 /4)	$P_{1/4}$	$4\alpha^{3/4}$	$\alpha^{1/4}$

2.4. Thermodynamic method

According to the activation energy calculated by FWO and KAS methods, the pre-exponential factor A, thermodynamic parameters such as enthalpy ΔH, Gibbs free energy ΔG, and entropy ΔS at a given heating rate can be calculated by the following equations [31,32].

$$A = \frac{\beta E \exp\left(\frac{E}{RT_m}\right)}{RT_m^2} \tag{9}$$

$$\Delta H = E - RT \tag{10}$$

$$\Delta G = E - RT_m \ln\left(\frac{K_B T_m}{hA}\right) \tag{11}$$

Preprints (www.preprints.org) | NOT PEER-REVIEWED | Posted: 26 June 2023 doi:10.20944/preprints202306.1739.v1

$$\Delta S = \frac{\Delta H - \Delta G}{T_m} \quad (12)$$

Here, T_m is the maximum decomposition temperature of DTG peak, K_B represents the boltzmann constant (1.381×10^{-23} J/K), and h is the Planck's constant (6.626×10^{-34} J/s).

3. Results

3.1. Thermogravimetric analysis

The TG and DTG curves of wheat straw at different heating rates are shown in Figure 3. The pyrolysis process of wheat straw can be divided into three stages: dehydration, main pyrolysis, and carbonization. The first stage (room temperature to 453 K) is the initial stage of pyrolysis, which is mainly the removal of water and some small molecules of volatile substances. When the heating rate is 10, 20, and 30 K/min, the weight loss is 8.69%, 8.71%, and 8.72%, respectively, which is very close to the water content in Table 1. The second stage (453 K to 773 K) is the main stage of the pyrolysis process. Since the biomass is mainly composed of hemicellulose, cellulose, and lignin [33], the hemicellulose, cellulose, and most lignin are pyrolyzed in this stage, and the shoulder and sharper peaks can be clearly seen on the DTG curve. The shoulder peak is related to the pyrolysis of hemicellulose and lignin, and the sharper peak is caused by the pyrolysis of cellulose and lignin of wheat straw. At the heating rates of 10, 20, and 30 K/min, the maximum pyrolysis rates are 7.92, 17.25, and 30.72 %/min, respectively. The third stage (773 K to 1,173 K) is the continuous decomposition of residual lignin, carbon precipitation, and ash formation. At this stage, less volatile components are released, and a slight weight loss can be seen. At the end of pyrolysis process, the residual masses are 17.65%, 17.58%, and 17.52% at different heating rates, respectively.

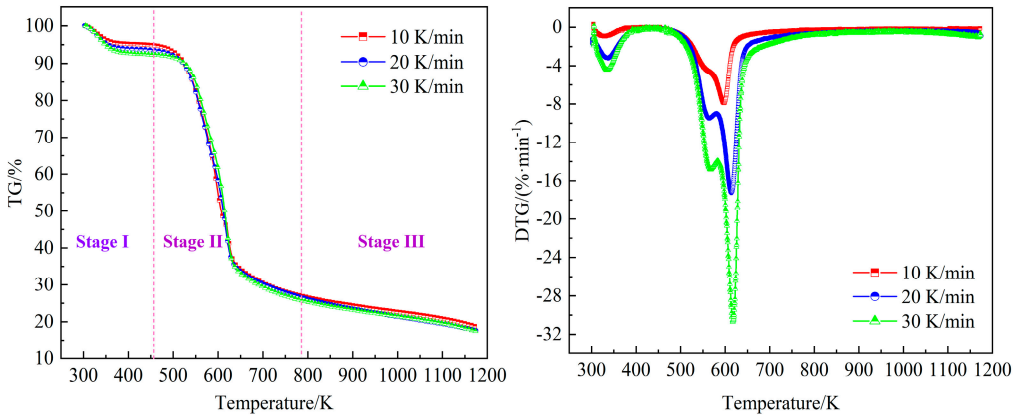

Figure 3. TG and DTG curves of pyrolysis process for wheat straw.

The characteristic parameters of the main pyrolysis stage were obtained by TG and DTG curves, as shown in Table 3. As can be seen from the Table 3, the heating rate has a little difference on the weight loss in the main pyrolysis stage. With increasing heating rate, the starting pyrolysis temperature of the main pyrolysis stage and the temperature corresponding to the weight loss peak gradually increased. This is because that at a higher heating rate, the rate of chemical bond breaking is fast, which is easy to produce volatile polymer materials, and thus increases the pyrolysis temperature. Within the same temperature range, the higher the heating rate, the shorter the residence time of wheat straw, which is not conducive to heat transfer, resulting in a larger temperature difference between the surface and the interior. Therefore, the overall pyrolysis DTG curve shifts to higher temperature.

Preprints (www.preprints.org) | NOT PEER-REVIEWED | Posted: 26 June 2023 doi:10.20944/preprints202306.1739.v1

Table 3. Characteristic parameters of the main pyrolysis stage.

Heating rates /(K/min)	Starting temperature/ K	Temperature of first shoulder peak/K	Temperature of second sharper peak/K	Ending temperature/ K	Percentage of weight loss/%
10	454.6	549.6	597.4	740.9	63.24
20	460.9	563.3	613.9	758.3	63.82
30	470.5	567.7	617.2	773.4	64.08

3.2. Kinetics analysis

Activation energy is the minimum amount of energy required for a molecule to change from normal to an active state, where a chemical reaction takes place. In order to improve the accuracy of the calculation results, the pyrolysis process with a conversion rate of 0.2–0.8 was analyzed. The linear correlations of the pyrolysis process fitted by FWO and KAS methods are shown in Figure 4.

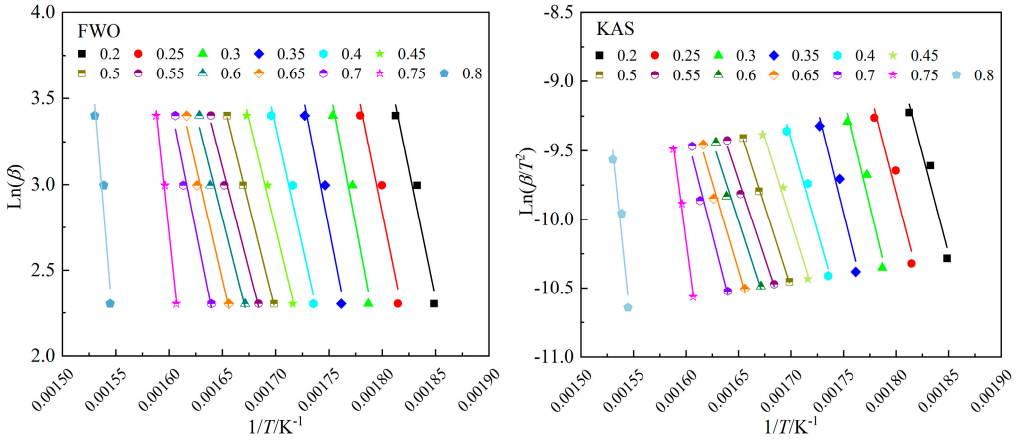

Figure 4. Pyrolysis kinetics fitted by FWO and KAS methods.

The kinetic parameters calculated by the two different methods are listed in Table 4. As can be seen from the Table 4, the correlation coefficients R^2 of FWO ($0.950<R^2<1$) and KAS ($0.941<R^2<1$) are both above 0.940, indicating the ideal linear fitting and high reliability of calculation results. The activation energy calculated by FWO and KAS methods range from 165.17 to 440.02 kJ/mol and 163.72 to 452.07 kJ/mol, and the average value are 223.59 kJ/mol and 225.33 kJ/mol, respectively.

Table 4. Kinetic parameters calculated by the two different methods.

α	FWO			KAS		
	E/(kJ/mol)	A/(1/s)	R^2	E/(kJ/mol)	A/(1/s)	R^2
0.20	184.00	1.27×10^{14}	0.952	184.46	1.40×10^{14}	0.949
0.25	181.24	7.20×10^{13}	0.950	181.39	7.42×10^{13}	0.941
0.30	201.28	4.52×10^{15}	0.951	202.33	5.61×10^{15}	0.951
0.35	195.62	1.40×10^{15}	0.954	196.23	1.59×10^{15}	0.951
0.40	184.10	1.30×10^{14}	0.974	183.95	1.26×10^{14}	0.972
0.45	181.90	8.24×10^{13}	0.990	181.51	7.60×10^{13}	0.989
0.50	190.82	5.21×10^{14}	0.999	190.86	5.26×10^{14}	0.999
0.55	171.52	9.61×10^{12}	0.991	170.46	7.73×10^{12}	0.990
0.60	165.17	2.58×10^{12}	0.978	163.72	1.91×10^{12}	0.976
0.65	182.89	1.01×10^{14}	0.982	182.27	8.91×10^{13}	0.980

Preprints (www.preprints.org) | NOT PEER-REVIEWED | Posted: 26 June 2023 doi:10.20944/preprints202306.1739.v1

0.70	203.96	7.85×10^{15}	0.973	204.34	8.50×10^{15}	0.971
0.75	424.12	2.92×10^{35}	0.994	435.75	3.12×10^{36}	0.994
0.80	440.02	7.45×10^{36}	0.958	452.07	8.66×10^{37}	0.950
Average	223.59			225.33		

The variation trend of activation energy upon conversion rate has been manifested in Figure 5. The activation energy obtained by FWO and KAS methods are similar, and the activation energy calculated by FWO method is slightly lower than that of KAS method. The trend of activation energy upon conversion rate can be divided into three stages: when the conversion rate is from 0.2 to 0.3, the activation energy begins to increase slightly, which is mainly due to the decomposition of hemicellulosic and cellulose of wheat straw. When the conversion rate is from 0.3 to 0.6, the activation energy shows a decreasing trend, which corresponds to the pyrolysis of cellulose of wheat straw. A large amount of volatile substances produced at this stage, and the semi-crystal structure of cellulose was destroyed, making the pyrolysis process easy to occur. When the conversion rate ranges from 0.6 to 0.8, the activation energy becomes to increase rapidly, especially when the conversion rate is above 0.7. This is mainly because that a large amount of lignin start to pyrolyze, and produce coke with low reactivity in this stage.

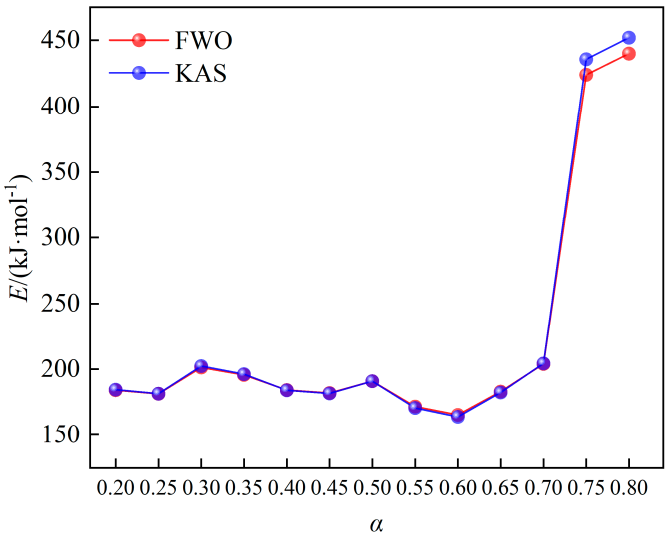

Figure 5. Variation trend of activation energy upon conversion rate.

The pre-exponential factor A is an important index reflecting the surface structure of the sample or the complexity of the reaction during pyrolysis. When the value of A is $<10^9$ s^{-1}, the reaction is the surface reaction; when the value of A is $\geq10^9$ s^{-1}, it means the occurrence of complex reaction [34]. As can be seen in Table 4, at the heating rate of 10 K/min, the pre-exponential factors calculated by FWO and KAS methods vary in the range of 2.58×10^{12} to 7.45×10^{36} s^{-1} and 1.91×10^{12} to 8.66×10^{37} s^{-1}, respectively. This indicates that the pyrolysis process of wheat straw involves multiple parallel reactions, and it is very complicated. The variation trend of the pre-exponential factor upon conversion rateis consistent with that of the activation energy.

3.3. Thermodynamic analysis

Thermodynamics analysis is in favor to study the energy changes in the pyrolysis process. The thermodynamics parameters, such as enthalpy ΔH, Gibbs free energy ΔG, and entropy ΔS along with the change trend upon the conversion rate at the heating rate of 10 K/min are shown in Table 5.

Preprints (www.preprints.org) | NOT PEER-REVIEWED | Posted: 26 June 2023 doi:10.20944/preprints202306.1739.v1

Table 5. Thermodynamic parameters of wheat straw calculated by KAS and FWO methods.

α	FWO			KAS		
	ΔH/(kJ/mol)	ΔG/(kJ/mol)	ΔS/(J/mol/K)	ΔH/(kJ/mol)	ΔG/(kJ/mol)	ΔS/(J/mol/K)
0.20	179.50	172.45	11.80	179.96	172.44	12.58
0.25	176.66	172.53	6.92	176.80	172.52	7.17
0.30	196.63	172.01	41.22	197.68	171.98	43.01
0.35	190.90	172.15	31.39	191.51	172.13	32.43
0.40	179.31	172.45	11.49	179.16	172.45	11.23
0.45	177.05	172.51	7.60	176.66	172.52	6.93
0.50	185.92	172.27	22.85	185.96	172.27	22.92
0.55	166.58	172.80	-10.42	165.53	172.83	-12.23
0.60	160.20	172.99	-21.41	158.74	173.03	-23.92
0.65	177.87	172.48	9.02	177.25	172.50	7.95
0.70	198.89	171.94	45.11	199.27	171.93	45.77
0.75	418.92	168.31	419.56	430.55	168.17	439.25
0.80	434.63	168.12	446.15	446.68	167.99	466.55
Average	218.70	171.77	78.56	220.44	171.75	81.51

Enthalpy represents the energy stored in the system. Change in enthalpy determines the loss or gain in energy of the system. Table 5 shows that the ΔH calculated by FWO and KAS methods vary in the ranges of 160.20 to 434.63 kJ/mol and 158.74 to 446.68 kJ/mol, and the average valule are 218.70 and 220.44 kJ/mol, respectively. The ΔH calculated by the two methods have the same trend upon the conversion, and both are positive, indicating that the parallel reaction involved in the pyrolysis process of wheat straw is dominated by the endothermic reaction. In addition, the difference between ΔH and E calculated by the two methods is about ±6 kJ/mol at the same conversion rate, implying that the pyrolysis process is highly reactive and easy to occur, which is conducive to the formation of activation complexes with low energy [35,36].

Gibbs free energy denotes the available energy of biomass that can be used for the chemical transformation along with the formation of activated complex. Table 5 shows that the ΔG calculated by FWO and KAS methods range from 168.12 to 172.99 kJ/mol and 167.99 to 173.03 kJ/mol, and the average value are 171.77 kJ/mol and 171.75 kJ/mol, respectively. In addition, the values of ΔG vary within ±5 kJ/mol corresponding to each conversion rate, indicating that wheat straw has a stable energy output during the whole pyrolysis process.

Entropy denotes molecular disorder and randomness of the system. Lower entropy may be related to physical changes or minor chemical reactions, while higher entropy indicates higher reactivity and the formation of activated complexes. Table 5 shows that the change in entropy calculated by FWO and KAS methods range from −21.41 to 446.68 J/(mol×K) and −23.92 to 466.55 J/(mol×K), respectively. The ΔS values calculated by the two methods were observed to be negative for the conversion rate 0.55–0.60, while positive values were shown for rest of the conversion rate. Where negative ΔS values implies that a thermally stable product is produced, and the thermodynamic equilibrium was established. Whereas, positive ΔS values indicates that the disorder degree of pyrolysis products was larger than that of initial reactants [37]. Especially, when the conversion rate is above 0.7, the entropy shows a large increase, indicating that the system has greater disorder and higher reaction activity at the end of the pyrolysis reaction, and the pyrolysis reaction is difficult to reach thermodynamic equilibrium [38].

According to the variation trend of the thermodynamic parameters upon the conversion rate in Table 5, it can clearly seen that the variation trend of ΔG is opposite to that of ΔH and ΔS. The values of ΔH and ΔS increase slightly when the conversion rate is 0.2 to 0.3. In this process, hemicelluloses

Preprints (www.preprints.org) | NOT PEER-REVIEWED | Posted: 26 June 2023 doi:10.20944/preprints202306.1739.v1

and cellulose in wheat straw begin to decompose gradually, and the disorder of the reaction system increases. This process corresponds to the first shoulder peak in the DTG curve of the second stage in Figure 3. When the conversion rate ranges from 0.3 to 0.6, the disorder of the system begins to decrease due to the gradual decomposition of hemicellulose and cellulose, and the values of ΔH and ΔS decrease gradually, which corresponds to the second weight loss sharper peak in the DTG curve. When the conversion rate varies from 0.6 to 0.8, the lignin of wheat straw begins to decompose and produce coke with low reactivity, thus the values of ΔH and ΔS increase significantly. The results of thermodynamic analysis show that the wheat straw has a massive quantity of inherent energy and potential to be exploited as a source for bioenergy production.

3.4. Reaction Mechanism

The CR method was employed to investigate the reaction mechanism during pyrolysis at a different level of conversion at a heating rate of 10 K/min. The reaction mechanisms selected are mentioned in Table 2. It is mainfested that the values of activation energy had a little fluctuation in the conversion range of 0.2–0.7, as shown in Table 4. While, the changes in activation energy were significant when the conversion rate is above 0.7. Therefore, the conversion range of 0.2–0.7, which is the main pyrolysis stage based on the primary analysiswas studied in detail. If the average activation energy values acquired by the discussed mechanism functions are almost equal to the energy values obtained from FWO and KAS methods, it indicates that this mechanism function should be the best-fit reaction mechanism of the main stage of the pyrolysis process.

After comparing the average activation energy E with that of the model-free methods obtained in the previous section, the detailed results are shown in Table 6. It is indicated that, the average E value (192.84 kJ/mol) calculated by the mechanism function $A_{1/3}$ ($g(\alpha) = [-\ln(1-\alpha)]^3$) corresponding to random nucleation mechanism is nearly equal to the value (185.68 kJ/mol^{-1} and 185.59 kJ/mol^{-1}) estimated based upon FWO and KAS methods in the conversion range of 0.2–0.7. The relative error is less than 4%, and the correlation coefficients R^2 exceeds 0.997. Therefore, it is credible that the $A_{1/3}$ random nucleation model is the optimal mechanism function to characterize the pyrolysis process. It implies that during the pyrolysis process in the conversion range of 0.2–0.7, the random nucleation may play a pivotal role.

Table 6. The activation energy calculated by the CR method in the conversion range of 0.2–0.7.

Mechanism	symbol	E/(kJ/mol)	R^2
One-way transport	D_1	91.96	0.999
Two-way transport	D_2	104.67	0.999
Three-way transport	D_3	119.97	0.998
Ginstling-Brounshtein	D_4	109.73	0.999
Zhuravlev,Lesokin,Tempelman	D5	153.69	0.993
First-order	F_1	62.74	0.995
Second-order	F_2	90.53	0.986
Third-order	F_3	123.99	0.977
Avrami-Erofeyev(n=2)	A_2	26.51	0.993
Avrami-Erofeyev(n=3)	A_3	14.43	0.991
Avrami-Erofeyev(n=4)	A_4	8.39	0.985
Avrami-Erofeyev(n=1/2)	$A_{1/2}$	128.68	0.997
Avrami-Erofeyev(n=1/3)	$A_{1/3}$	192.84	0.997
Avrami-Erofeyev(n=1/4)	$A_{1/4}$	266.92	0.997
Contracting disk	R_1	40.99	0.999
Contracting cylinder	R_2	51.119	0.998

Preprints (www.preprints.org) | NOT PEER-REVIEWED | Posted: 26 June 2023 doi:10.20944/preprints202306.1739.v1

Contracting sphere	R_3	54.829	0.997
Power law (n = 1 /2)	P_2	15.649	0.997
Power law (n = 1 /3)	P_3	7.169	0.993
Power law (n = 1 /4)	P_4	2.93	0.975
Averageactivation energy(0.2–0.7)	FWO	185.68 kJ/mol	
	KAS	185.59 kJ/mol	

4. Conclusions

In this work, the pyrolysis behavior of wheat straw were identified using TGA experiments. The kinetic parameters of pyrolysis at three different heating rates, and the thermodynamics parameters at the heating rate of 10 K/min were obtained using the model-free methods (FWO and KAS). Meanwhile, the reaction mechanism was determined by the model-fitting method (CR).

The following conclusions are drawn:

- The thermogravimetric analysis results show that there are three main weight loss stages in the pyrolysis of wheat straw. The first stage is the drying and dehydration stage, the second stage is the main pyrolysis stage, and the third stage is the continuous decomposition and carbonization of residual lignin. With increasing heating rate, the DTG curve of pyrolysis shifts to higher temperature.
- The activation energy calculated by FWO and KAS methods are 165.17–440.02 kJ/mol and 163.72–452.07 kJ/mol, respectively. The pre-exponential factors obtained by FWO and KAS methods are in the range of 2.58×10^{12}–7.45×10^{36} s^{-1} and 1.91×10^{12}–8.66×10^{37} s^{-1} at the heating rate of 10 K/min. The change trend of pre-exponential factor is consistent with that of activation energy.
- The variation trend of thermodynamic parameters ΔG upon conversion rate is opposite to that of ΔH and ΔS during wheat straw pyrolysis. Thermodynamic analysis shows that the potential energy barrier between ΔE and ΔH is about 6 kJ/mol, indicating the favorable conditions for product formation. The wheat straw contains a massive quantity of inherent energy to be exploitedas a source for bioenergy production.
- It was found that the mechanism function $A_{1/3}$ ($g(\alpha) = [-\ln(1-\alpha)]^3$) is the most suitable mechanism function to characterize the main pyrolysis stage. Random nucleation may be in charge of the pyrolysis process in the conversion range of 0.2–0.7.

Author Contributions: Conceptualization, J.L.; formal analysis, J.L. and D.Z.; investigation, X.Y.; data curation, X.Y. and H.W.; writing—original draft preparation, J.L.; writing—review and editing, J.L. and H.W.; supervision, D.Z. All authors have read and agreed to the published version of the manuscript.

Funding: This research was funded by the Opening Foundation of The State Key Laboratory of Refractories and Metallurgy (Wuhan University of Science and Technology), grant number G202208, and the Key project of Hubei Polytechnic University, grant number 21xjz01A.

Institutional Review Board Statement: Not applicable.

Informed Consent Statement: Not applicable.

Data Availability Statement: Not applicable.

Acknowledgments: The authors gratefully acknowledge the resources partially provided by the State Key Laboratory of Refractories & Metallurgy, Wuhan University of Science and Technology.

Conflicts of Interest: The authors declare no conflicts of interest.

References

1. Martin, A.D. Co-development of a tool to aid the assessment of biomass potential for sustainable resource utilization : An exploratory study with Danish and Swedish municipalities. *Sustainability* **2023**, *15*, 9772.
2. Estefan, L.; Carlos, M.; Saparrat, N. Potentials of biomass waste valorization : Case of south America. *Sustainability* **2023**, *15*, 8343.
3. Zou, R.G.; Qian, M.; Wang, C.X.; Mateo, W.; Wang, Y.P.; Dai, L.L.; Lin, X.N.; Zhao, Y.F.; Huo, E.G.; Wang, L.; Zhang, X.S.; Kong, X.; Ruan, R.; Lei, H.W. Biochar : From by-products of agro-industrial lignocellulosic waste to tailored carbon-based catalysts for biomass thermochemical conversions. *Chem. Eng. J.* **2022**, *441*, 135972.
4. Thanapal, S.S.; Annamalai, K.; Sweeten, J.M.; Gordillo, G. Fixed bed gasification of dairy biomass with enriched air mixture. *Appl. Energ.* **2012**, *97*, 525.
5. Ertas, M.; Alma, M.H. Pyrolysis of laurel (Laurus nobilis L.) extraction residues in a fixed-bed reactor : Characterization of bio-oil and bio-char. *J. Anal. Appl. Pyrol.* **2010**, *88*, 22.
6. Aon, M.; Aslam, Z.; Hussain, S.; Bashir, M.A.; Shaaban, M.; Masood, S.; Iqbal, S.; Khalid, M.; Rehim, A.; Mosa, W.F.A.; Sas-Paszt, L.; Marey, S.A.; Hatamleh, A.A. Wheat Straw biochar produced at a low temperature enhanced maize growth and yield by influencing soil properties of typic calciargid. *Sustainability* **2023**, *15*, 9488.
7. Uras, Ü.; Carrier, M.; Hardie, A.G.; Knoetze, J.H. Physico-chemical characterization of biochars from vacuum pyrolysis of South African agricultural wastes for application as soil amendments. *J. Anal. Appl. Pyrol.* **2012**, *98*, 207.
8. Yuan, X.S.; He, T.; Cao, H.L.; Yuan, Q.X. Cattle manure pyrolysis process: kinetic and thermodynamic analysis with isoconversional methods. *Renew. Energ.* **2017**, *107*, 489.
9. Vijayan, S.K.; Kibria, M.A.; Uddin, H.; Bhattacharya, S. Pretreatment of automotive shredder residues , their chemical characterisation , and pyrolysis kinetics. *Sustainability* **2021**, *13*, 10549.
10. Manić, N.; Janković, B.; Dodevski, V. Model-free and model-based kinetic analysis of Poplar fluff (Populus alba) pyrolysis process under dynamic conditions. *J. Therm. Anal. Calorim.* **2021**, *143*, 3419.
11. Yao, Z.T.; Yu, S.Q.; Su, W.P.; Wu, W.H.; Tang, J.H.; Qi, W. Kinetic studies on the pyrolysis of plastic waste using a combination of model-fitting and model-free methods. *Waste Manage. Res.* **2020**, *38*, 77.
12. Fetisova, O.Y.; Mikova, N.M.; Taran, O.P. Evaluation of the validity of model-fitting and model-free methods for kinetic analysis of nonisothermal pyrolysis of Siberian fir bark. *Kinet. Catal.*, **2020**, *61*, 846.
13. Ravari, F.; Noori, M.; Ehsani, M. Thermal stability and degradation kinetic studies of PVA/RGO using the model-fitting and Isoconversional (model-free) methods. *Fiber. Polym.* **2019**, *20*, 472.
14. Khiari, B.; Jeguirim, M. Pyrolysis of grape marc from Tunisian wine industry: Feedstock characterization, thermal degradation and kinetic analysis. *Energies* **2018**, *11*, 730.
15. Galiwango, E.; Al-Marzuoqi, A.H.; Khaleel, A.A.; Abu-Omar, M.M. Investigation of non-Isothermal kinetics and thermodynamic parameters for the pyrolysis of different date palm parts. *Energies* **2020**, *13*, 6553.
16. Radhakumari, M.; Prakash, D.J.; Satyavathi, B. Pyrolysis characteristics and kinetics of algal biomass using TGA analysis based on ICTAC recommendations. *Biomass Conv. Bioref.* **2016**, *6*, 189.
17. Vyazovkin, S.; Burnham, A.K.; Favergeon, L.; Koga, N.; Moukhina, E.; P'erez-Maqueda, L.A.; Sbirrazzuoli, N. ICTAC kinetics committee recommendations for analysis of multi-step kinetics. *Thermochim. Acta* **2020**, *689*, 178597.
18. Singh, S.; Chakraborty, J.P.; Mondal, M.K. Intrinsic kinetics, thermodynamic parameters and reaction mechanism of non-isothermal degradation of torrefied acacia nilotica using isoconversional methods. *Fuel* **2020**, *259*, 116263.
19. Tao, W.M.; Zhang, P.; Yang, X.W.; Li, H.; Liu, Y.; Pan, B. An integrated study on the pyrolysis mecanism of peanut shell based on the kinetic analysis and solid/gas characterization. *Bioresour. Technol.* **2021**, *329*, 124860.
20. Inayat, A.; Fagieh, T.M.; Esraa, M. Kinetics and thermodynamic study of calligonum polygonoides pyrolysis using model-free methods. *Process Saf. Environ.* **2022**, *1160*, 130.
21. Nawaz, A.; Kumar, P. Elucidating the bioenergy potential of raw, hydrothermally carbonized and torre fi ed waste arundo donax biomass in terms of physicochemical characterization, kinetic and thermodynamic parameters. *Renew. Energ.* **2022**, *187*, 844.
22. Mishra, R.K.; Mohanty, K. Characterization of non-edible lignocellulosic biomass in terms of their candidacy towards alternative renewable fuels. *Biomass Convers. Bior.* **2018**, *8*, 799.
23. Rammohan, D.; Kishore, N.; Uppaluri, R.V.S. Insights on kinetic triplets and thermodynamic analysis of delonix regia biomass pyrolysis. *Bioresour. Technol.* **2022**, *358*, 127375.
24. Choudhury, D.; Borah, R.C.; Goswamee, R.L.; Sharmah, H.P.; Rao, P.G. Non-isothermal thermogravimetric pyrolysis kinetics of waste petroleum refinery sludge by isoconversional approach. *J. Therm. Anal. Calorim.* **2007**, *89*, 965.
25. Ahmad, M.S.; Mehmood, M.A.; Ayed, O.S. Kinetic analyses and pyrolytic behavior of para grass (Urochloa mutica) for its bioenergy potential. *Bioresour. Technol.* **2017**, *224*, 708.

26. Coats, A.W.; Redfern, J. Kinetic parameters from thermogravimetric data. *Nature* **1964**, *201*, 68.
27. Coats, A.W.; Redfern, J. Kinetic parameters from thermogravimetric data II. *J. Polym. Sci. C Polym. Lett.* **1965**, *3*, 91.
28. Vlaev, L.; Nedelchev, N.; Gyurova, K.; Zagorcheva, M. A comparative study of non-isothermal kinetics of decomposition of calcium oxalate monohydrate. *J. Anal.Appl. Pyrol.* **2008**, *81*, 253.
29. Jiang, H.Y.; Wang, J.G.; Wu, S.Q.; Wang, B.S.; Wang, Z.Z. Pyrolysis kinetics of phenol-formaldehyde resin by non-isothermal thermogravimetry. *Carbon* **2010**, *48*, 352.
30. Chen, R.Y.; Li, Q.W.; Xu, X.K.; Zhang, D.D.; Hao, R.L. Combustion characteristics, kinetics and thermodynamics of pinus sylvestris pine needle via non-isothermal thermogravimetry coupled with model-free and model-fitting methods. *Case Stud. Therm. Eng.* **2020**, *22*, 100756.
31. Kaur, R.; Gera, P.; Jha, M.K.; Bhaskar, T. Pyrolysis kinetics and thermodynamic parameters of castor (Ricinus communis) residue using thermogravimetric analysis. *Bioresour. Technol.* **2017**, *250*, 422.
32. Dong, R.H.; Chen, F.J.; Zhang, F.X.; Yang, S.L.; Liu, H.L.; Wang, H.; Hu, J.H. A comprehensive evaluation on pyrolysis kinetics, thermodynamics , product properties and formation pathways of jatropha oil for high-value utilization. *Fuel* **2022**, *313*, 122982.
33. Wang, S.S.; Zou, C.; Lou, C.; Yang, H.P.; Jing, H.X.; Cheng, S.Z. Effects of hemicellulose, cellulose and lignin on the ignition behaviors of biomass in a drop tube furnace. *Bioresour. Technol.* **2020**, *310*, 123456.
34. Shahid, A.; Ishfaq, M.; Ahmad, M. S.; Malik, S.; Farooq, M.; Hui, Z.; Batawi, A.H.; Shafi, M.E.; Aloqbi, A.A.; Gull, M.; Mehmood, M.A. Bioenergy potential of the residual microalgal biomass produced in city wastewater assessed through pyrolysis, kinetics and thermodynamics study to design algal biorefinery. *Bioresour. Technol.* **2019**, *289*, 121701.
35. Patidar, K.; Singathia, A.; Vashishtha, M.; Sangal, V.K.; Upadhyaya, S. Investigation of kinetic and thermodynamic parameters approaches to non-isothermal pyrolysis of mustard stalk using model-free and master plots methods. *Mater. Sci. Energy Technol.* **2021**, *5*, 6.
36. Chen, J.B.; Wang, Y.H.; Lang, X.M.; Ren, X.E.; Fan, S.S. Evaluation of agricultural residues pyrolysis under non-isothermal conditions : Thermal behaviors, kinetics, and thermodynamics. *Bioresour. Technol.* **2017**, *241*, 340.
37. Petrovič, A.; Vohl, S.; Cenčič Predikaka, T.; Bedoić, R.; Simonič, M.; Ban, I.; Čuček, L. Pyrolysis of solid digestate from sewage sludge and lignocellulosic biomass: Kinetic and thermodynamic analysis, characterization of biochar. *Sustainability* **2021**, *13*, 9642.
38. Singh, S.; Patil, T.; Tekade, S.P.; Gawande, M.B.; Sawarkar, A.N. Studies on individual pyrolysis and co-pyrolysis of corn cob and polyethylene : Thermal degradation behavior, possible synergism, kinetics, and thermodynamic analysis. *Sci. Total Environ.* **2021**, *783*, 147004.